Journal of
Computational and Theoretical Nanoscience
Vol. 10, 1–9, 2013

Optimal Approach Trajectories for a Hydrogen Donation Tool in Positionally Controlled Diamond Mechanosynthesis

Denis Tarasov[1], Ekaterina Izotova[1], Diana Alisheva[1], Natalia Akberova[1], and Robert A. Freitas, Jr[2,*]

[1] *Kazan Federal University, Department of Biochemistry, Kazan, Tatarstan, 420008, Russia*
[2] *Institute for Molecular Manufacturing, Palo Alto, CA 94301, USA*

The use of precisely applied mechanical forces to induce site-specific chemical transformations is called positional mechanosynthesis, and diamond is an important early target for achieving mechanosynthesis experimentally. A key step in diamond mechanosynthesis (DMS) may employ a Ge-substituted adamantane-based hydrogen donation tool (HDon) for the site-specific mechanical hydrogenation of depassivated diamond surfaces. This paper presents the first theoretical study of DMS tool-workpiece operating envelopes and optimal tool approach trajectories for a positionally controlled hydrogen donation tool during scanning-probe based UHV diamond mechanosynthesis. Trajectories were analyzed using Density Functional Theory (DFT) in PC-GAMESS at the B3LYP/6-311G(d, p)//B3LYP/3-21G(2d, p) level of theory. The results of this study help to define equipment and tooltip motion requirements that may be needed to execute the proposed reaction sequence experimentally and provide support for early developmental targets as part of a comprehensive near-term DMS implementation program.

Keywords: Adamantane, Carbon, Diamond, DMS, Donation, Germanium, Hydrogen, Mechanosynthesis, Nanotechnology, Positional Control, Reaction Sequence, Trajectory.

RESEARCH ARTICLE

1. INTRODUCTION

Arranging atoms in most of the ways permitted by physical law is a fundamental objective of molecular manufacturing. A more modest and specific objective is the ability to synthesize atomically precise diamondoid structures using positionally controlled molecular tools. Such positional control might be achieved using an instrument like a Scanning Probe Microscope (SPM). The landmark experimental demonstration of positional atomic assembly occurred in 1989 when Eigler and Schweizer[1] employed an SPM to spell out the IBM logo using 35 xenon atoms arranged on nickel surface, though no covalent bonds were formed. The use of precisely applied mechanical forces to induce site-specific chemical transformations using positionally-controlled highly reactive tools in nonreactive environments such as UHV is called positional diamond mechanosynthesis (DMS).[2,3] Positional mechanosynthesis has been demonstrated experimentally for Si, Ge, Sn, Pb and In,[4–6] and C mechanosynthesis is being efforted.[7] The stability of intermediate structures arising during the mechanosynthesis of diamond has also received support from recent theoretical work.[8,9]

A key step in the process of atomically precise mechanosynthetic fabrication of diamond is to add a hydrogen atom to a radical site at a specific lattice location on the diamond surface, passivating that site using a positionally controlled reaction step. This additional could be done using a hydrogen donation tool[2] that has a modest chemical affinity for hydrogen at one end but is elsewhere inert. The tool's unreactive region serves as a handle or handle attachment point. The tool would be held by a high-precision nanoscale positioning device such as an SPM tip that is moved directly over particular radical sites on a diamond workpiece surface. One suitable molecule for a hydrogen donation tooltip is the Group IV-bridgehead-substituted adamantane such as the germanium-substituted adamantane (1,1-germano-adamantane) (Fig. 1) that is brought up to a partially dehydrogenated diamond surface (Fig. 2(A)) or bridgehead-dehydrogenated adamantane

*Author to whom correspondence should be addressed.

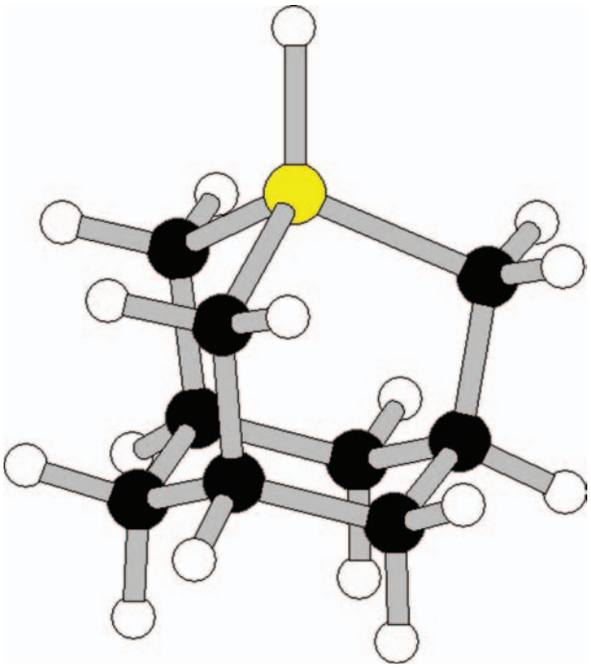

Fig. 1. The germanium-substituted adamantane (1,1-germano-adamantane) tooltip "HDon" for hydrogen donation, from Freitas and Merkle (2008).[2] (C = black, H = white, Ge = yellow).

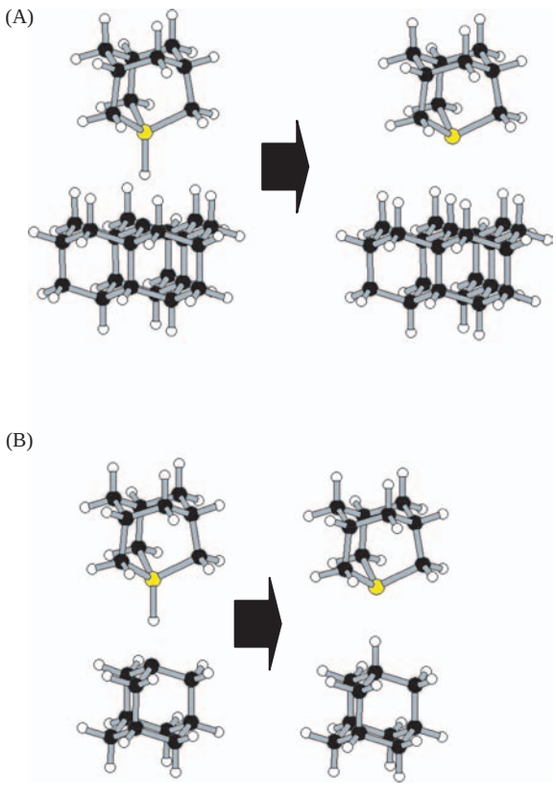

Fig. 2. Exemplar hydrogen donation reactions in which a hydrogen atom is transferred from the HDon to (A) a C (111) diamond surface or (B) a bridgehead-depassivated adamantane molecule, from Freitas and Merkle (2008).[2] (C = black, H = white, Ge = yellow).

RESEARCH ARTICLE

cage (Fig. 2(B)) as a site-specific active tool and then is retracted as a spent tool from a now-passivated diamond workpiece.[2] It is this latter reaction that we study in the present work. The HDon tool is readily covalently bonded to a larger handle structure by extension of a regular diamond lattice of which the adamantane base is a unit cage. The environment around the tool would be inert (e.g., vacuum or a noble gas such as xenon).

The radical chemistry of H donation has been studied[10–15] but only recently have such tools been investigated theoretically using the tools of computational chemistry. The first high-quality analysis of the Ge-based HDon tool operating on small cluster targets by Temelso et al.[16] reports H donation from a Ge-substituted isobutane model tooltip to an sp^3 carbon monoradical recipient site (isobutane model) to be exoergic by $\Delta E = -0.62$ eV at the CCSD(T)/DZ-PP level of theory with a +0.21 eV reaction barrier calculated at the UMP2/DZ-PP level of theory. Based on bending potentials calculated at the MP2/cc-pVDZ[-PP] level of theory, positional uncertainty of the donor H atom is estimated to be < 0.22 Å at 298 K or one-tenth the ~ 2.5 Å spacing between potential donation sites on an unreconstructed C(111) diamond surface, thus allowing adequate positional control during the donation operation.

Site-specific hydrogen donation to crystal surfaces, but not purely mechanical donation, has been achieved experimentally. For instance, McIntyre et al.[17] demonstrated nanocatalytic capabilities of a platinum-rhodium STM tip operating in a reactor cell with excess H_2 by rehydrogenating partially dehydrogenated hydrocarbon clusters adsorbed to the Pt (111) surface. Muller et al.[18] used a Pt-coated AFM tip to hydrogenate terminal azide groups on a self-assembled monolayer, producing highly localized amines. Huang and Yamamoto[19] demonstrated the deposition of hydrogen atoms from an STM tungsten tip to a monohydride Si(100)–H(2 × 1) surface by applying a +3.5 V voltage bias to diffuse the hydrogens to the tungsten tip, followed by −8.5 V 300 ms pulses to induce electronic excitations to break the W—H bond. Thirstrup et al.[20] used clean and H-coated STM tips to perform atomic scale desorption and deposition of hydrogens from Si(001)–H(2 × 1) and Si(001)–H(3 × 1) surfaces for both positive and negative sample bias voltages with a resolution of one to two atomic rows.

While the proposed donation reaction sequence appears energetically favorable, to date the positional and rotational operating envelopes of specific hydrogen donation tools acting on specific surfaces, workpieces, or other tools have not been examined theoretically. This paper presents the first theoretical study of a tool-workpiece operating envelope for a hydrogen donation tool during scanning-probe based ultrahigh-vacuum diamond mechanosynthesis. The results of this study help to define equipment and tooltip motion requirements that may be needed to execute the proposed reaction sequence experimentally

and provide guidance on early development targets as part of a comprehensive near-term DMS implementation program.

2. COMPUTATIONAL METHODS

All studies were conducted using Density Functional Theory (DFT) in the PC-GAMESS version[21] of the GAMESS (US) QC package[22] running on a computational cluster consuming ∼106,800 CPU-hours of runtime at 1 GHz, and included 2,620 separate valid-structure calculations. The work was performed primarily at the Kazan Branch of the Joint Supercomputer Center at the Russian Academy of Sciences of RAS using the MVS100KF system consisting of 80 nodes with 2 Quad Core Intel Xeon E5450 (3 GHz) processors per node. A few additional computations were performed using four Intel Core i7 based desktop computers at Kazan Federal University. As in previous work,[3] all energies were calculated with the 6-311G(d, p)//3-21G(2d, p) basis set using B3LYP which is a hybrid Hartree-Fock/DFT method using Becke's three-parameter gradient-corrected exchange functional (B3)[23] with the Lee–Yang–Parr correlation functional (LYP).[24] Zero-point corrections are not made to the energy data because:

(1) the differences between energies with and without a correction are small,

(2) the number of points to be evaluated is large (many thousands in this study), and

(3) the computational expense is huge (e.g., analytical second derivatives for spin-unrestricted calculations are not implemented in PC-GAMESS and the calculation of numerical frequencies requires about twice as much CPU time as geometry optimizations).

The present work examines the positionally controlled mechanosynthetic reaction in which a hydrogen donation tool (HDon) donates a single hydrogen atom to a carbon atom at a radical site on an adamantane cage workpiece at (1) a bridgehead position (Fig. 2(B)) and (2) a sidewall position. The HDon tool and the adamantane cage workpiece are constrained by fixing the positions of the three sidewall carbon atoms (CH_2 groups) in the tooltip adamantane base that are located on the side of the cage farthest from the active radical site of the tool, and the similar atoms in the base of the adamantane cage workpiece. Each tool and workpiece were thus fixed precisely in space by constraining just 3 base atoms in each structure from the start of each run, then the system was allowed to relax to its equilibrium geometry during the run. This method provides the best model for anticipated actual laboratory conditions in which an experimentalist will control tooltip position by applying forces through a larger diamond lattice handle structure affixed behind the base structure of the tooltip. For each run, each tooltip base was positionally constrained to a specific spherical coordinate

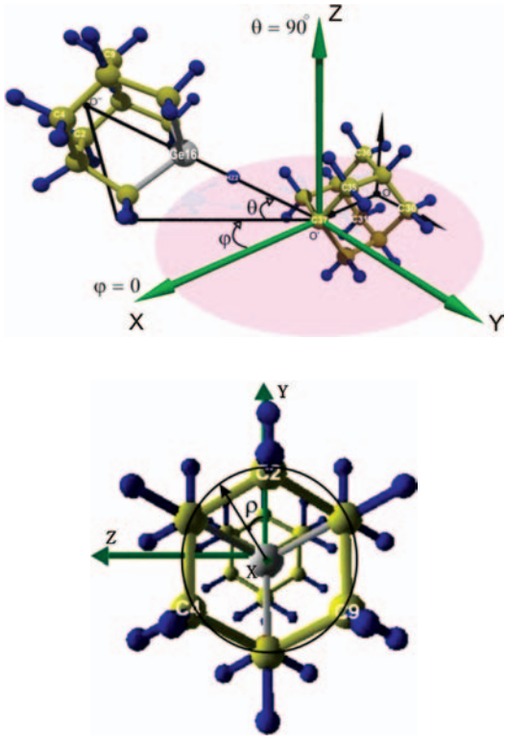

Fig. 3. Above: Coordinate system definition for the positionally controlled donation of hydrogen atom H22 to adamantane bridgehead radical site at carbon atom C37, defining phi (φ) and theta (θ), including atom labels; drawing shows system positioned at approximately (φ, θ, ρ) = (+30°, +30°, 0°). Below: Definition of the tooltip axial rotation angle rho (ρ), below, with the X-axis (green dot) pointing out of the page. (C = yellow, H = blue, Ge = gray).

φ (in XY plane) and θ (in Z direction) in fixed increments, and to several fixed radial distances R, and the incoming tooltip was also constrained to a specific axial rotational angle ρ.

The tooltip geometry and coordinate system for the bridgehead donation reaction is shown in Figure 3. The first coordinate origin O is defined as the point equidistant from the fixed carbon atoms C30, C31, and C36 in the workpiece adamantane base, and lying in the plane containing those atoms. The X axis lies perpendicular to the C30/C31/C36 plane and points from origin O to a second origin O′ which is initially coincident with atom C37 in the adamantane base, 2.592 Å away from O. The Y axis originates at O′, lies perpendicular to the X axis, and runs parallel to a vector pointing from origin O to atom C30. The Z axis also originates at O′ and lies perpendicular to X and Y axes following the right-hand rule, running parallel to a vector pointing from atom C31 to atom C36. The approaching HDon tool is initially oriented relative to the adamantane workpiece such that a line extending backwards through atoms C37 (origin O′) and germanium atom Ge16 perpendicularly penetrates the plane defined by the 3 fixed HDon tool base carbon atoms (C2, C4, and C9), intersecting a third origin O″ which lies in the C2/C4/C9

RESEARCH ARTICLE

plane and is equidistant from C2, C4 and C9, analogous to origin O.

In this spherical coordinate system, φ is defined as the angle from the X axis to the Y axis of the projection of the vector pointing from O′ to O″ onto the XY plane. Note that $+\varphi$ is defined as rotation toward the $-Y$ axis in the arrow direction and θ is defined as the angle from the XY plane to the vector pointing from O′ to O″, with $-180° \leq \varphi \leq +180°$ and $-90° \leq \theta \leq +90°$. Tool-workpiece separation distance R is defined as the distance between origins O″ and O′. Although atom C37 moves away from O′ as the reaction proceeds, the proper experimental protocol is nevertheless to aim the O″-to-Ge16 vector directly toward the fixed origin O′ (not to C37, which moves) to execute the reaction. The rotational state of the adamantane workpiece is completely specified after labeling the base atoms C30, C31, and C36 and defining the positive Y-axis as the O-to-C30 direction. The rotational state of HDon, specified by ρ, is measured as the angle taken from the O-to-C31 vector to the O″-to-C2 vector when HDon is virtually repositioned to $(\varphi, \theta) = (180°, 0°)$ making O″ coincident with O, with $+\rho$ taken in the clockwise direction as viewed from O′. Thus, rotation to $+\varphi$ becomes equivalent to rotation to $-\rho$ at $\theta = +90°$, or to $+\rho$ at $\theta = -90°$. This coordinate system was chosen because origins O and O″ experience negligible reaction-mediated nonthermal displacement during the course of the reaction and thus may be most directly controlled in an experimental apparatus.

The tooltip geometry and coordinate system for the sidewall donation reaction is the same as for the bridgehead case except that the coordinate origin O′ is translated from the bridgehead carbon atom C37 to the sidewall carbon atom C35 while maintaining the existing Cartesian axis orientation, after first adding a hydrogen atom to passivate the bridgehead atom C37 and removing a hydrogen atom from sidewall atom C35 to create a new target radical site on the adamantane workpiece. This method facilitates easier comparison of the two sets of PES maps.

3. RESULTS AND DISCUSSION

3.1. Hydrogen Donation to Bridgehead Site

For a positionally controlled H atom donation from an HDon tool to a bridgehead radical position on an adamantane workpiece, Figure 4 shows the 1D PES as a function of tool-workpiece separation distance R for a simple $(\varphi, \theta, \rho) = (0°, 0°, 0°)$ trajectory using mostly 0.1 Å step sizes, but adding a 0.05 Å step before and after the transfer distance. This PES indicates that hydrogen atom transfer occurs exoergically by −0.50 eV at R = 6.1 Å after the incoming HDon tool surmounts a minimum barrier height of +0.16 eV, results that are very consistent with the +0.21 eV barrier and −0.62 eV transfer favorability previously estimated by Temelso et al. (2007).[16]

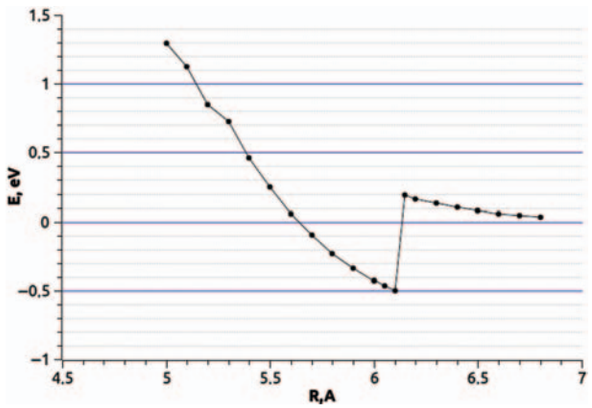

Fig. 4. 1D PES for hydrogen donation from HDon to a bridgehead radical site on an adamantane workpiece, at $(\varphi, \theta, \rho) = (0°, 0°, 0°)$ using 0.1 Å and 0.05 Å step sizes.

The angular deviation of H22 from collinearity with the O″-Ge16-O′ line, ranging from 0.4° pre-transfer to 1.0°–1.4° post-transfer for a $(\varphi, \theta, \rho) = (0°, 0°, 0°)$ trajectory, suggests that only small lateral forces are imposed on the transfer H atom while traversing the barrier.

Figure 5 shows the 2D PES for the same positionally controlled reaction at R = 5.9 Å, 6.0 Å, 6.1 Å and 6.2 Å for approach trajectories in the range $(\varphi, \theta, \rho) = (\pm 60°, \pm 70°, 0°)$. Each PES only includes points where the distance between any two opposing atoms in tool and workpiece is > 1 Å; tool-workpiece positions that fail this condition (deemed to be "in collision") or which suffer pathological rearrangements are excluded the PES. The largest possible exoergic range for trajectories in which the HDon tool is applied to this workpiece appears to be $(\varphi, \theta) \approx (\pm 40°, \pm 40°)$, although $(\varphi, \theta) = (\pm 30°, \pm 30°)$ is probably required for reliable room temperature operation. An additional 42 points extending out to $\varphi = -100°$ and $+130°$ at $R = 5.9$ Å and 54 points out to $\varphi = -180°$ and $+150°$ at $R = 6.1$ Å, for $\theta = \pm 70°$ (not shown in the charts), confirm that the outlying regions of the PES remain solidly endoergic.

Another important criterion for successful completion of a positionally controlled mechanosynthetic reaction is the minimization of energy barriers. If the activation energy for a selected approach trajectory is too high, the tools may not be able to deliver sufficient force to compel the reaction to go forward, or the tool or workpiece might suffer unacceptably large flexures during their attempt to overcome a high barrier, potentially opening the door to additional trajectory or reaction pathologies. Figure 6 shows the positional location of the maximum barrier and the maximum energy barrier height for hydrogen donation from an HDon tool to a bridgehead radical site on an adamantane workpiece, at tool-workpiece separation distances $R = 6.0 - 6.2$ Å using approach trajectories in the range $(\varphi, \theta, \rho) = (\pm 60°, \pm 70°, 0°)$. The reaction barrier is a minimum using a $(\varphi, \theta) = (\pm 10°, \pm 10°)$

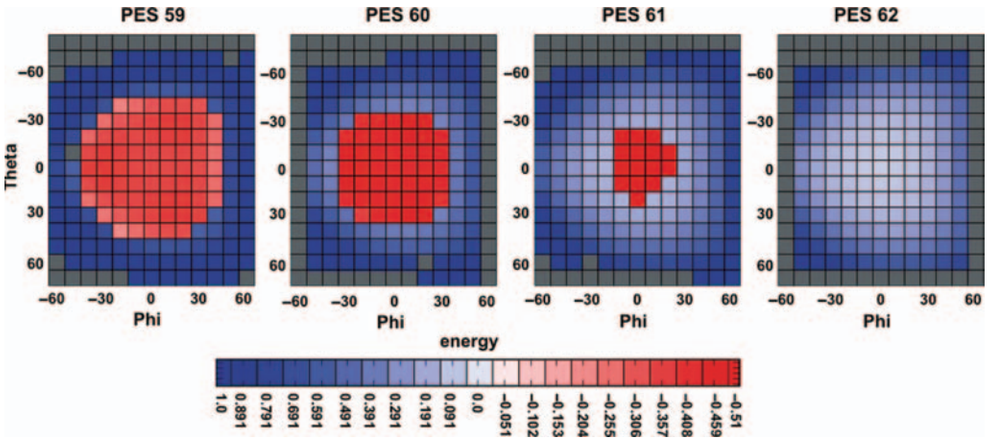

Fig. 5. 2D PES (endoergic = blue, exoergic = red, excluded = gray) at tool-workpiece separation distances $R = 5.9$–6.2 Å using approach trajectories in the range $(\varphi, \theta, \rho) = (\pm 60°, \pm 70°, 0°)$ spanning the H transfer position, for hydrogen donation from HDon to a bridgehead radical site on an adamantane workpiece.

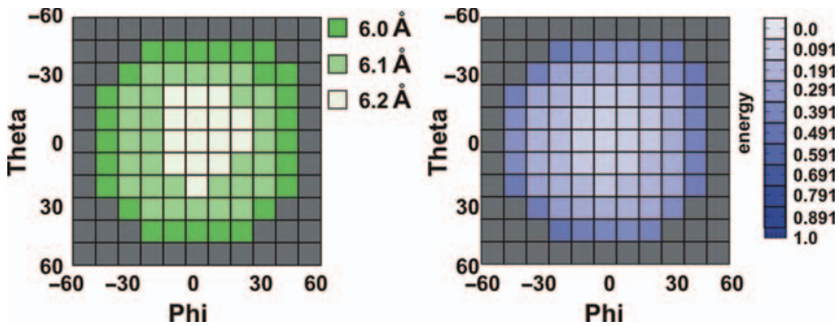

Fig. 6. Positional location of maximum barrier (left) and the maximum energy barrier height (right) for hydrogen donation from an HDon tool to a bridgehead radical site on an adamantane workpiece, at tool-workpiece separation distances $R = 6.0$–6.2 Å using approach trajectories in the range $(\varphi, \theta, \rho) = (\pm 60°, \pm 70°, 0°)$.

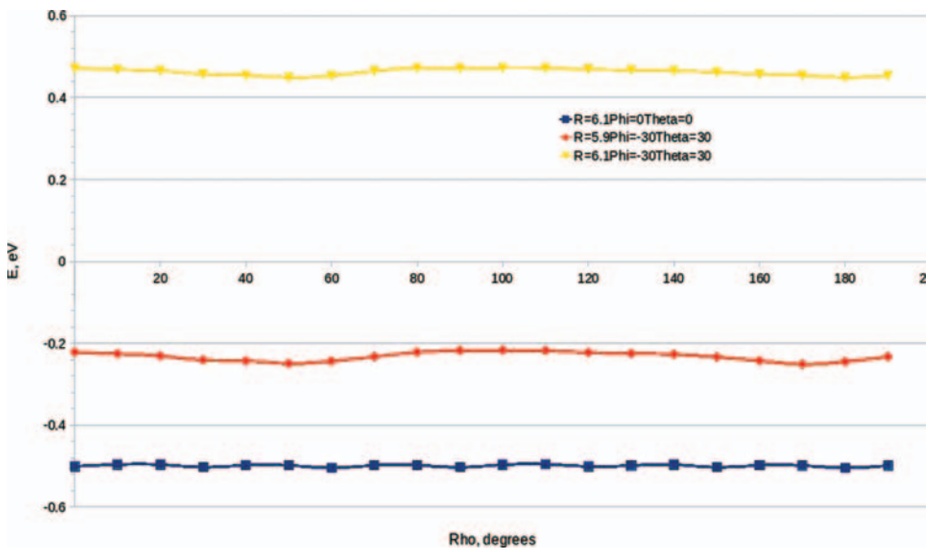

Fig. 7. Effect of tooltip rotational angle ρ on PES for hydrogen donation from an HDon tool to a bridgehead radical site on an adamantane workpiece.

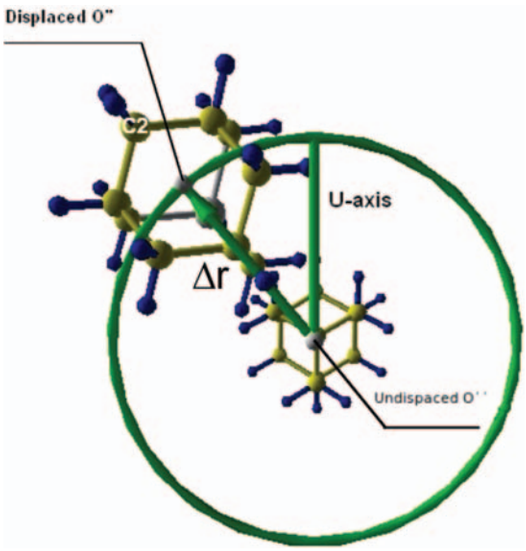

Fig. 8. Geometry used for displacement error tolerance with HDon shown at left and the adamantane workpiece bridgehead radical target site shown at right, in position to consummate the donation reaction, with O″ radically displaced from its original location by a distance Δr. (C = yellow, H = blue, Ge = gray).

trajectory where transfer occurs at $R = 6.1$ Å, rising by $0.05 - 0.10$ eV for $(\varphi, \theta) = (+20°/+30°, +20°/+30°)$ trajectories where transfer occurs at $R \sim 6.0$ Å, and reaching a maximum of 0.30–0.40 eV for the most highly angled viable trajectories at $(\varphi, \theta) = (+40°, +40°)$ where transfer occurs at $R \sim 5.9$ Å. Thus the transfer distance decreases slightly and the barrier increases markedly for high angle approach trajectories.

Figure 7 shows that HDon tooltip rotational angle ρ has little effect on the PES for hydrogen transfer from the HDon tool to the bridgehead radical site of an adamantane workpiece. Using the simplest $(\varphi, \theta) = (0°, 0°)$ trajectory, at the transfer distance for this reaction ($R = 6.1$ Å) the PES has a negligible ± 0.008 eV variation in reaction favorability with changing ρ because the HDon tool and the adamantane workpiece are maximally distant, thus minimizing steric interactions. But even using a fairly high-angled trajectory such as $(\varphi, \theta) = (-30°, +30°)$ the pre-transfer PES still has a negligible ± 0.023 eV variation with ρ at $R = 6.1$ Å and a post-transfer variation of ± 0.031 eV with ρ at $R = 5.9$ Å. The two major dips in these last two curves lie 120° apart and are attributable to the symmetrical tripartite tool geometry around the bridgehead atom of the HDon tool and the adamantane workpiece; other minor anomalies are low in energy and well within the range of computational uncertainty.

To specify a useful experimental protocol it is also necessary to determine the maximum tolerable lateral misplacement error of HDon that will still result in a successful consummation of the donation reaction. We start by defining the U-axis as a vector pointing from O″ to C2 and the V-axis as a vector originating at O″ and perpendicular to U that points parallel and codirectional with a vector from C9 to C4 (Fig. 8). We can then examine whether the H donation still occurs when HDon is translationally displaced within the UV plane away from its intended position at any point within a particular approach trajectory. We define Δr as the radial displacement of O″ from its original location, in the UV plane. Simulations began by examining small Δr and moving to larger Δr, exploring progressively larger displacement error circles. At some Δr we would expect to find that H22 and C37 are too far apart to form the desired bond. The results of these tests indicate that for a $(\varphi, \theta, \rho) = (0°, 0°, 0°)$ trajectory at $R = 6.1$ Å, the H donation reaction fails at a displacement of $\Delta r \geq 0.6$ Å. At $R = 5.9$ Å, the donation reaction fails for a $(\varphi, \theta, \rho) = (0°, 0°, 0°)$ trajectory with a displacement of $\Delta r \geq 1.1$ Å, but fails at only $\Delta r \geq 0.5$ Å for a more highly angled $(\varphi, \theta, \rho) = (-30°, +30°, 0°)$ trajectory. Thus the tolerance for lateral displacement error in tool positioning decreases markedly for high angle approach trajectories, and an experimental system with 50–110 pm positional control is likely required to perform this mechanosynthetic reaction reliably.

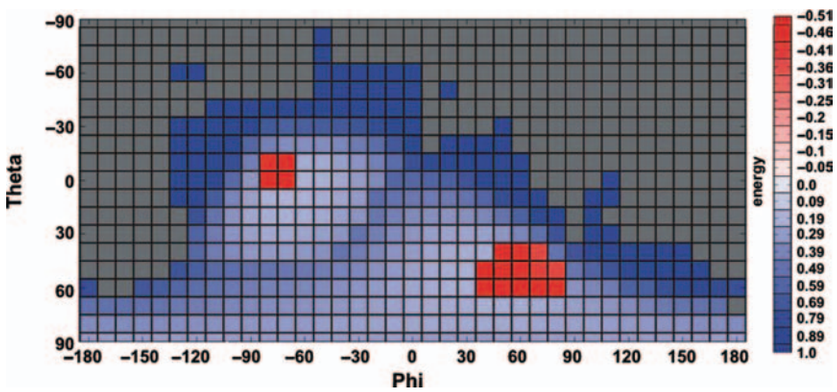

Fig. 9. 2D PES (endoergic = blue, exoergic = red, excluded = gray) at a pre-transfer tool-workpiece separation distance $R = 6.2$ Å using approach trajectories in the range $(\varphi, \theta, \rho) = (\pm 180°, \pm 90°, 0°)$ for hydrogen donation from HDon to a sidewall radical site on an adamantane workpiece.

RESEARCH ARTICLE

3.2. Hydrogen Donation to Sidewall Site

For a positionally controlled H atom donation from an HDon tool to a sidewall radical position on an adamantane workpiece, Figure 9 shows the 2D PES at the pre-transfer tool-workpiece separation distance $R = 6.2$ Å for approach trajectories in the range $(\varphi, \theta, \rho) = (\pm 180°, \pm 90°, 0°)$. Figure 10 shows the same PES at $R = 6.1$ Å and Figure 11 shows the PES at $R = 5.9$ Å, again for approach

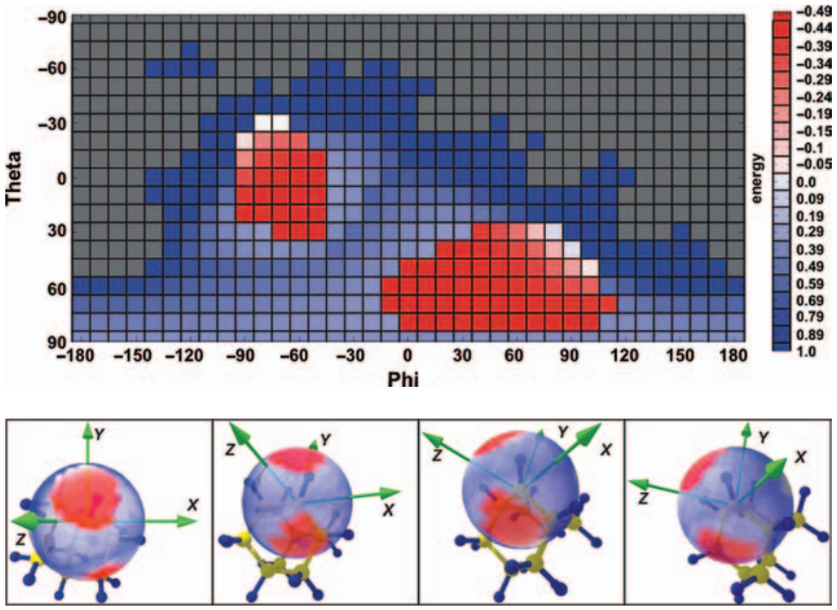

Fig. 10. 2D PES (endoergic = blue, exoergic = red, excluded = gray) at the tool-workpiece H-transfer separation distance $R_t = 6.1$ Å using approach trajectories in the range $(\varphi, \theta, \rho) = (\pm 180°, \pm 90°, 0°)$ for hydrogen donation from HDon to a sidewall radical site on an adamantane workpiece (top); at bottom, spherical representations of the smoothed PES as a function of tooltip positional angles expressed on a Cartesian XYZ coordinate system overlay the adamantane workpiece with targeted radical carbon atom C35 and its remaining hydrogen atom visible at center.

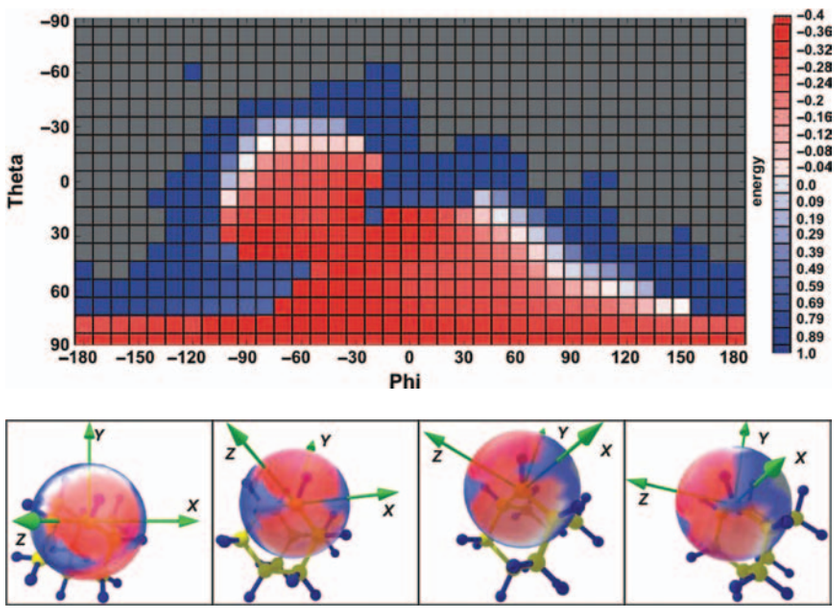

Fig. 11. 2D PES (endoergic = blue, exoergic = red, excluded = gray) at a tool-workpiece post-transfer separation distance $R = 5.9$ Å using approach trajectories in the range $(\varphi, \theta, \rho) = (\pm 180°, \pm 90°, 0°)$ for hydrogen donation from HDon to a sidewall radical site on an adamantane workpiece (top); at bottom, spherical representations of the smoothed PES as a function of tooltip positional angles expressed on a Cartesian XYZ coordinate system overlay the adamantane workpiece with targeted radical carbon atom C35 and its remaining hydrogen atom visible at center.

RESEARCH ARTICLE

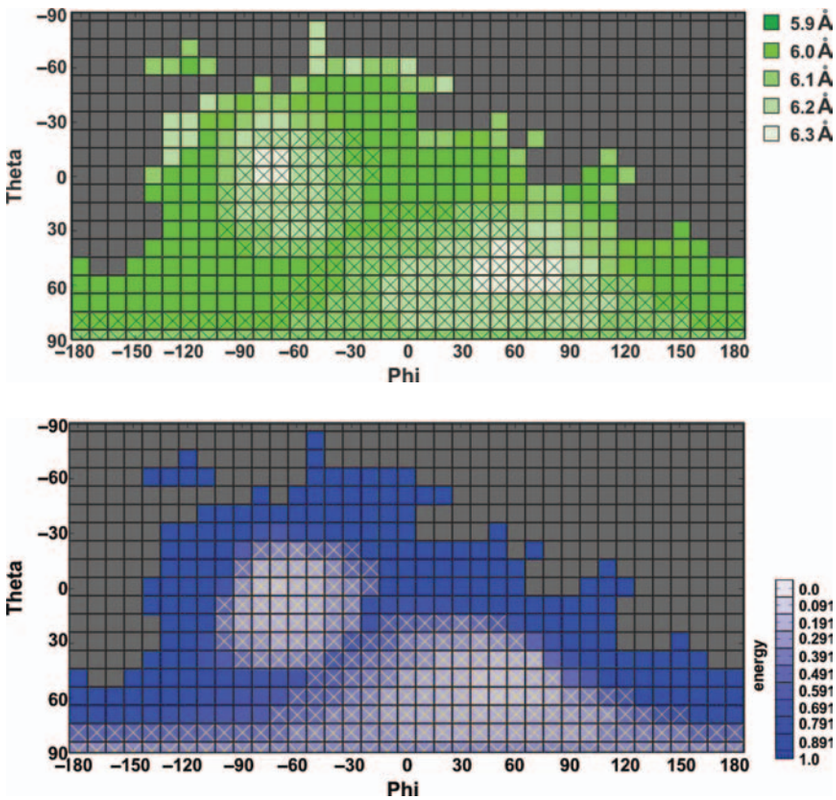

Fig. 12. Positional location of maximum barrier (top) and the maximum energy barrier height (bottom) for hydrogen donation from an HDon tool to a sidewall radical site on an adamantane workpiece, at tool-workpiece separation distances $R = 5.9 - 6.3$ Å using approach trajectories in the range $(\varphi, \theta, \rho) = (\pm 180°, \pm 180°, 0°)$ with successful hydrogen transfer trajectories marked (X).

RESEARCH ARTICLE

trajectories in the range $(\varphi, \theta, \rho) = (\pm 180°, \pm 90°, 0°)$, with spherical representations of the PES provided for clarity with both charts. As before, each PES only includes points where tool and workpiece are not in collision (distance between all opposed atoms in tool and workpiece lie > 1 Å apart) and have suffered no pathological rearrangements. These charts indicate that there are two exoergic approach trajectories, a smaller region near $(\varphi, \theta, \rho) = (-70°, 0°, 0°)$ and a larger region near $(\varphi, \theta, \rho) = (+50°, +60°, 0°)$. Respectively, these two exoergic regions expand the size of the viable angular trajectory windows from approximately $\pm 5°$ and $\pm 15°$ at $R = 6.2$ Å, to approximately $\pm 25°$ and $\pm 35°$ at $R = 6.1$ Å. These two regions are separated by a narrow endoergic ridge that represents the steric repulsion of the remaining H atom on the targeted carbon radical atom C35 that must be moved aside to complete the donation reaction. By $R = 5.9$ Å, these two exoergic islands have merged into one large energetically favorable region, filling in the entire slightly endoergic (light blue) areas in Figure 9 with exoergic trajectory space in Figure 11. This larger area provides at least some selection of exoergic trajectories for any φ between $\pm 180°$ and for any θ between $-10°$ to $+90°$, with viable trajectories continuously available throughout the $(\varphi, \theta) = (-30°$ to $-50°$, $-10°$ to $+90°)$ range.

Figure 12 shows the positional location of the maximum barrier and the maximum energy barrier height for hydrogen donation from an HDon tool to a sidewall radical site on an adamantane workpiece, at tool-workpiece separation distances $R = 5.9$–6.3 Å using approach trajectories in the range $(\varphi, \theta, \rho) = (\pm 180°, \pm 180°, 0°)$. The reaction barrier is a global minimum in the negative quadrant (upper left) at $+0.244$ eV using a $(\varphi, \theta) = (-70°, 0°)$ trajectory where transfer occurs at $R = 6.3$ Å, and is a local minimum in the positive quadrant (lower right) at $+0.246$ eV using a $(\varphi, \theta) = (+50°, +60°)$ trajectory where transfer occurs at $R = 6.2$ Å. Reaction barriers remain relatively low ($< +0.3$ eV) for a roughly $\pm 30°$ region around $(\varphi, \theta) = (-70°, +10°)$ and $(+50°, +60°)$, reaching a maximum of $+0.89$ eV for the most highly angled viable trajectories where H transfer occurs between $R \sim 5.9$–6.0 Å.

We also examined the maximum tolerable lateral misplacement error of HDon that will still result in a successful consummation of the donation reaction to the sidewall site. The results of these tests indicate that for a near-optimal $(\varphi, \theta, \rho) = (60°, 60°, 0°)$ trajectory at $R = 6.1$ Å, the H donation reaction fails at a displacement of $\Delta r \geq 0.6$ Å, again suggesting that an experimental system with ~ 50 pm positional control may be required to perform this mechanosynthetic reaction reliably.

4. CONCLUSIONS

The use of precisely applied mechanical forces to induce site-specific chemical transformations is called positional mechanosynthesis, and diamond is an important early target for achieving mechanosynthesis experimentally. A key step in diamond mechanosynthesis (DMS) may employ a Ge-substituted adamantane-based hydrogen donation tool (HDon) for the site-specific mechanical hydrogenation of depassivated diamond surfaces, thus eliminating a radical site that would otherwise remain chemically active and thereby stabilizing the workpiece. In this paper we undertake the first theoretical study of tool-workpiece operating envelopes and optimal tooltip trajectories for a positionally controlled hydrogen donation tool during scanning-probe based UHV diamond mechanosynthesis. The results of our study may help to define equipment and tooltip motion requirements that are needed to execute the proposed reaction sequence experimentally.

The optimal approach trajectory with minimum reaction barrier for a positionally controlled H atom donation from an HDon tool to a bridgehead radical position on an adamantane workpiece is a simple $(\varphi, \theta, \rho) = (0°, 0°, 0°)$ trajectory, where hydrogen atom transfer occurs exoergically by -0.50 eV at $R = 6.1$ Å after the incoming HDon tool surmounts a minimum barrier height of $+0.16$ eV. The largest possible exoergic range for trajectories in which the HDon tool is applied to this workpiece appears to be $(\varphi, \theta) \approx (\pm 40°, \pm 40°)$, although $(\varphi, \theta) = (\pm 30°, \pm 30°)$ is probably required for reliable room temperature operation; tool rotation angle ρ has little effect on reaction energetics. The barrier is a minimum of $+0.162$ eV using a $(\varphi, \theta) = (0°, 0°)$ trajectory where transfer occurs at $R =$ 6.1 Å, rising to $+0.18$ eV at $(\varphi, \theta) = (+10°, +10°)$ and reaching a maximum of $+0.56$ eV for the most highly angled viable trajectories at $(\varphi, \theta) = (+40°, +40°)$ where transfer occurs at $R \sim 5.9$ Å. The H donation reaction fails for a $(\varphi, \theta, \rho) = (0°, 0°, 0°)$ trajectory at a lateral misplacement error of $\Delta r \geq 0.6$ Å for $R = 6.1$ Å and at $\Delta r \geq$ 1.1 Å for $R = 5.9$ Å, but fails at $\Delta r \geq 0.5$ Å for a more highly angled $(\varphi, \theta, \rho) = (-30°, +30°, 0°)$ trajectory at $R = 5.9$ Å.

The optimal approach trajectory with minimum reaction barrier for a positionally controlled H atom donation from an HDon tool to a sidewall radical position on an adamantane workpiece is twofold: a smaller region near $(\varphi, \theta, \rho) = (-70°, 0°, 0°)$ and a larger region near $(\varphi, \theta, \rho) = (+50°, +60°, 0°)$. Respectively, these two exoergic regions expand the size of the viable angular trajectory windows from approximately $\pm 5°$ and $\pm 15°$ at $R = 6.2$ Å, to approximately $\pm 25°$ and $\pm 35°$ at $R = 6.1$ Å. By $R = 5.9$ Å, there is one large exoergic region providing at least some selection of exoergic trajectories for any φ between $\pm 180°$ and for any θ between $-10°$ to $+90°$, with viable trajectories continuously available throughout the $(\varphi, \theta) = (-30°$ to $-50°$, $-10°$ to $+90°)$ range. The reaction barrier has minimums for $(\varphi, \theta) = (-70°, 0°)$ and $(+50°, +60°)$ trajectories, and reaction barriers remain relatively low ($< +0.3$ eV) for a roughly $\pm 30°$ region around $(\varphi, \theta) = (-70°, +10°)$ and $(+50°, +60°)$. The H donation reaction fails for a $(\varphi, \theta, \rho) = (60°, 60°, 0°)$ trajectory at a lateral misplacement error of $\Delta r \geq 0.6$ Å for $R = 6.1$ Å.

References

1. D. M. Eigler and E. K. Schweizer, *Nature* 344, 524 (**1990**).
2. R. A. Freitas, Jr, and R. C. Merkle, *J. Comput. Theor. Nanosci.* 5, 760 (**2008**).
3. D. Tarasov, N. Akberova, E. Izotova, D. Alisheva, M. Astafiev, and R. A. Freitas Jr, *J. Comput. Theor. Nanosci.* 7, 325 (**2010**).
4. N. Oyabu, O. Custance, I. Yi, Y. Sugawara, and S. Morita, *Phys. Rev. Lett.* 90, 176102 (**2003**).
5. N. Oyabu, O. Custance, M. Abe, and S. Moritabe, *Abstracts of Seventh International Conference on Non-Contact Atomic Force Microscopy*, Seattle, Washington, USA, September (**2004**), vol. 34, pp. 12–15.
6. Y. Sugimoto, P. Pou, O. Custance, P. Jelinek, M. Abe, R. Perez, and S. Morita, *Science* 322, 413 (**2008**).
7. P. Moriarty, Digital Matter: Towards Mechanised Mechanosynthesis, EPSRC Fellowship Proposal (**2008**).
8. D. Tarasov, E. Izotova, D. Alisheva, N. Akberova, and R. A. Freitas Jr, *J. Comput. Theor. Nanosci.* 8, 147 (**2011**).
9. D. Tarasov, E. Izotova, D. Alisheva, N. Akberova, and R. A. Freitas, Jr, *J. Comput. Theor. Nanosci.* 9, 144 (**2012**).
10. E. Srinivasan, H. Yang, and G. N. Parsons, *J. Chem. Phys.* 105, 5467 (**1996**).
11. S. Sugahara, K. Hosaka, and M. Matsumura, *App. Surf. Sci.* 130, 327 (**1998**).
12. C. Chatgilialoglu, M. Ballestri, J. Escudie, and I. Pailhous, *Organometallics* 18, 2395 (**1999**).
13. L. Song, W. Wu, K. Dong, P. C. Hiberty, and S. Shaik, *J. Phys. Chem. A* 106, 11361 (**2002**).
14. T. I. Drozdova and E. T. Denisov, *Kinet. Catal.* 43, 10 (**2002**).
15. J. Olander and K. M. E. Larsson, *Thin Solid Films* 458, 191 (**2004**).
16. B. Temelso, C. D. Sherrill, R. C. Merkle, and R. A. Freitas Jr, *J. Phys. Chem. A* 111, 8677 (**2007**).
17. B. J. McIntyre, M. Salmeron, and G. A. Somorjai, *Science* 265, 1415 (**1994**).
18. W. T. Muller, D. L. Klein, T. Lee, J. Clarke, P. L. McEuen, and P. G. Schultz, *Science* 268, 272 (**1995**).
19. D. H. Huang and Y. Yamamoto, *Appl. Phys. A* 64, R419 (**1997**).
20. C. Thirstrup, M. Sakurai, T. Nakayama, and M. Aono, *Surf. Sci.* 411, 203 (**1998**).
21. Alex A. Granovsky, PC-GAMESS version 7. 1 www http://classic. chem. msu. su/gran/gamess/index. html (Some computations used version 7. 0), (**2009**).
22. M. W. Schmidt, K. K. Baldridge, J. A. Boatz, S. T. Elbert, M. S. Gordon, J. H. Jensen, S. Koseki, N. Matsunaga, K. A. Nguyen, S. Su, T. L. Windus, M. Dupuis, and J. A. Montgomery, *J. Comput. Chem.* 14, 1347 (**1993**).
23. A. D. Becke, *J. Chem. Phys.* 98, 5648 (**1993**).
24. C. Lee, W. Yang, and R. G. Parr, *Phys. Rev. B.* 37, 785 (**1988**).

Received: 11 February 2013. Accepted: 24 February 2013.